CHAPTER VIII
CONCLUSIONS

8.1 The Effects of Varying Feed Inlet Temperature

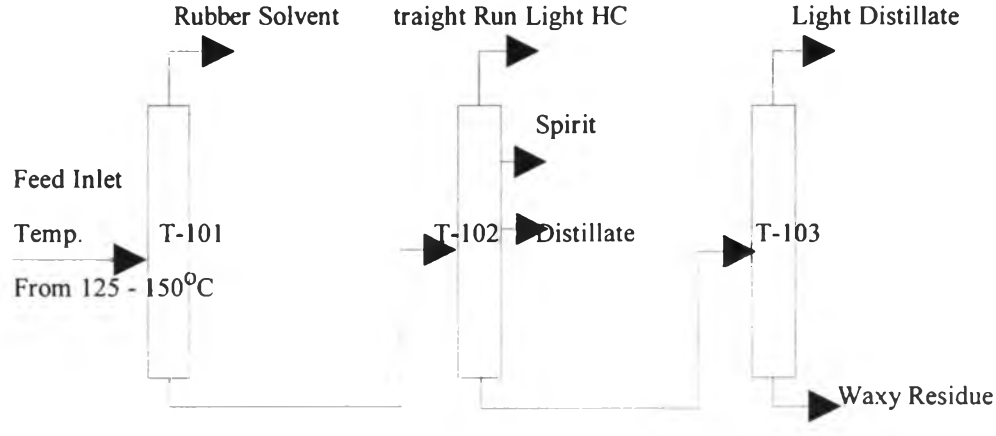

Figure 8.1 Flow diagram of refinery

8.1.1 The Effects of Varying Feed Inlet Temperature on Rubber Solvent (T-101)

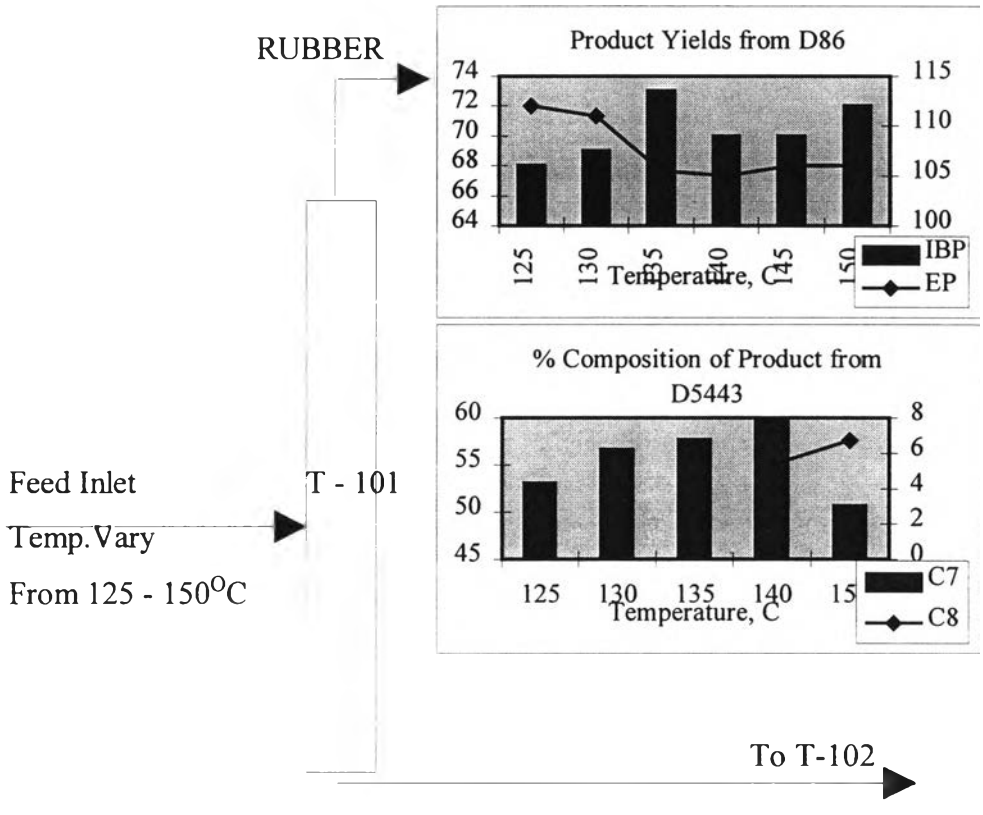

Figure 8.2 Drawing of T-101.

As shown in Figure 8.2 for product yields from D86, the IBP of Rubber solvents increased with increasing feed inlet temperature. This resulted in a heavier fraction of drawn product at the top of the column. But increasing the temperature of the feed inlet would result in a higher temperature at the top of column and a higher reflux temperature. This resulted in the reflux's inability to control the light fraction maintained in the column, so that the EP was decreased.

According to second of Figure 8.2 for percent composition of the product from D5443, the dominant component of Rubber solvent is C_7 which

increased until the feed inlet temperature was equal to 140°C after which C_7 was shifted down but correlated to C_8 was shifted up. Similar to the result from D86, the higher feed inlet temperature correlated to a heavier fraction of product.

8.1.2 The Effects of Varying Feed Inlet Temperature on Straight Run Light Hydrocarbon (Top of T-102)

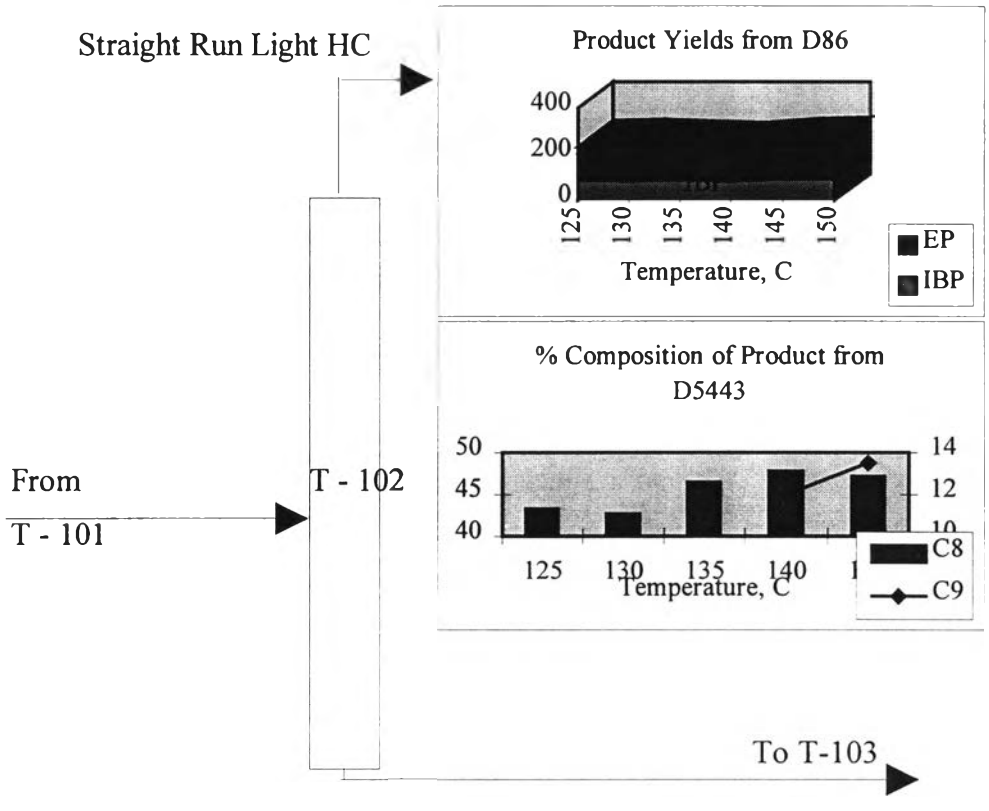

Figure 8.3 Drawing of T-102 (Top of T-102).

Based on GC analysis (ASTM D5443), the main component of Straight Run Light Hydrocarbon is C_8 hydrocarbon. Similarly, Rubber solvent IBP and EP correlated well with increasing feed inlet temperature.

8.1.3 The Effects of Varying Feed Inlet Temperature on Spirit (First Side Draw of T-102)

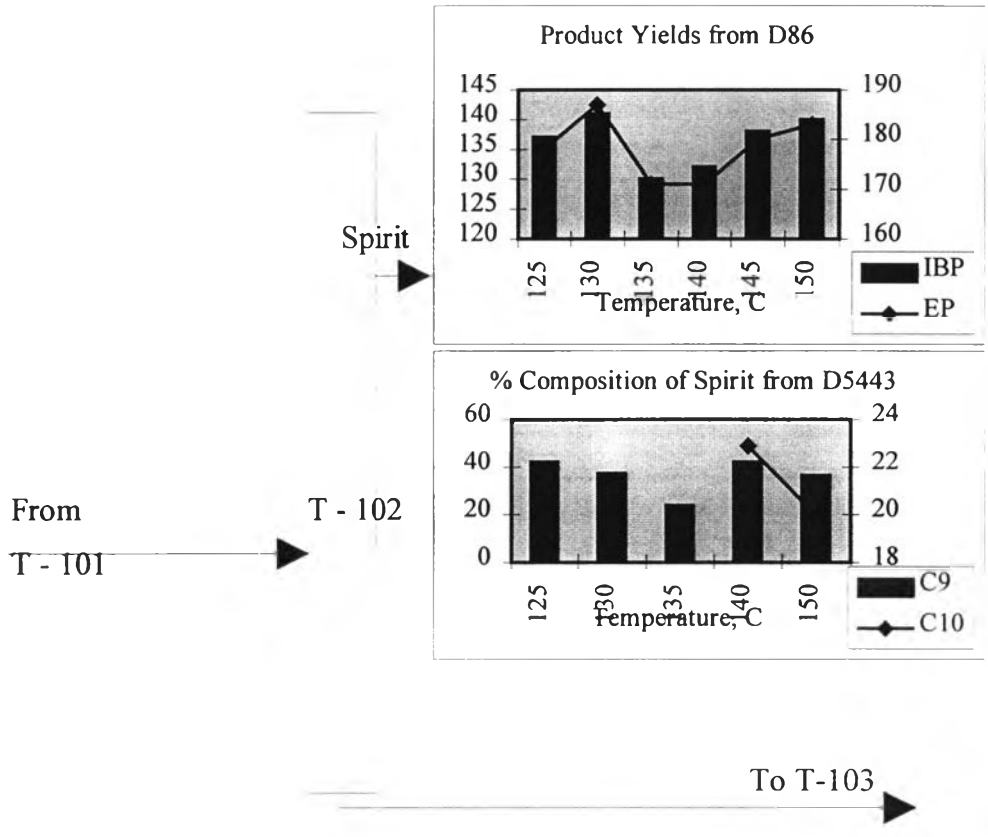

Figure 8.4 Drawing of T-102 (First Side Draw).

As shown in Figure 8.4, the dominant component of Spirit is C_9. Similarly with Rubber solvent, IBP and EP correlated well with increasing feed inlet temperature.

Accordingly, the percent composition of Spirit from D5443 C_9 and C_{10} was decreased. This is probably the result of the increased feed inlet temperature above the boiling point of C_9 and C_{10}, or might shifted from hydrocarbons greater than C_{11}, but ASTM D5443 was not able to be performed on hydrocarbon greater than C_{11}.

8.1.4 The Effects of Varying Feed Inlet Temperature on Distillate (Second Side Draw of T-102)

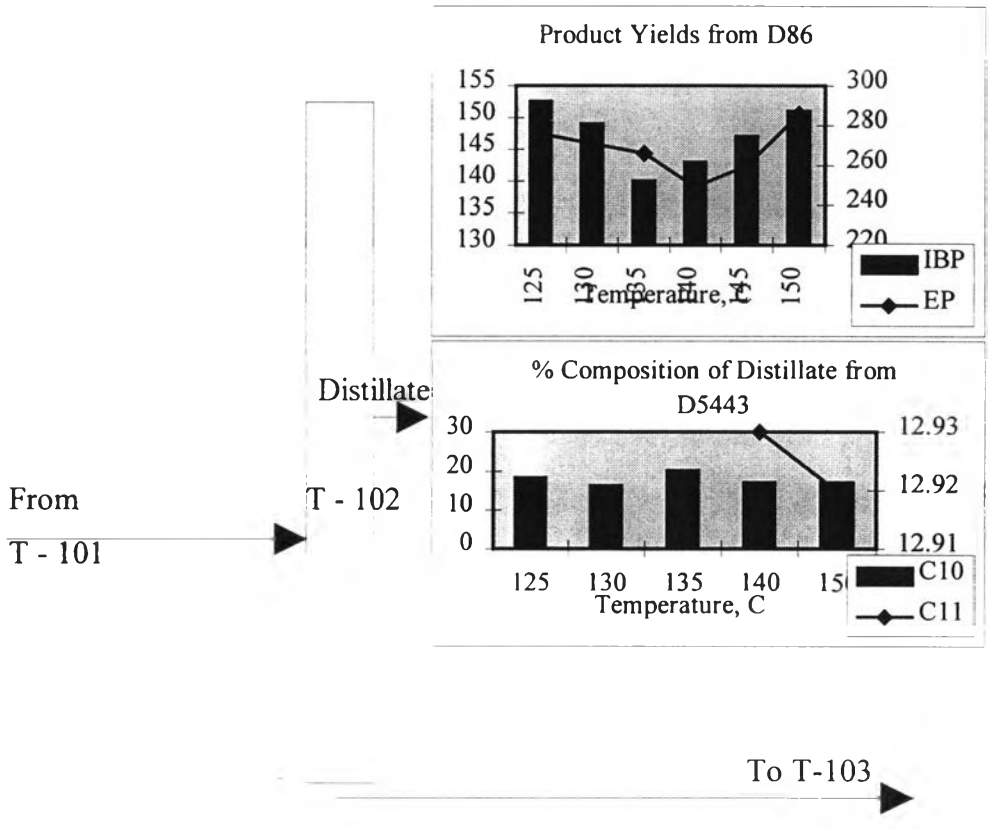

Figure 8.5 Drawing of T-102 (Second Side Draw).

Based on GC analysis (ASTM D5443), the main component of Distillate is C_{10} hydrocarbon. Similarly with Spirit (First Side Draw), IBP and EP correlated well with increasing feed inlet temperature.

8.1.5 The Effects of Varying Feed Inlet Temperature on Light Distillate (T-103)

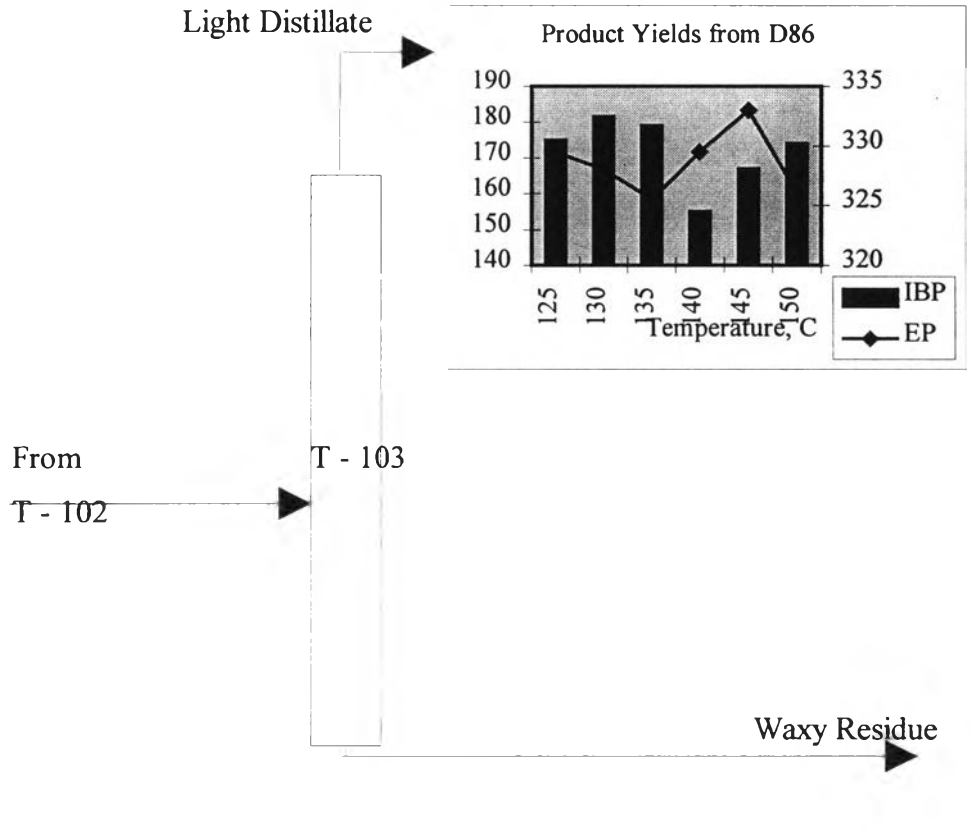

Figure 8.6 Drawing of T-103.

As shown in Figure 8.6, there would appear to be no observable trends for IBP and EP's with increasing feed inlet temperature. The influence of the furnace might be less for the third tower, from which the Light Distillate was obtained.

8.2 The Effects of Varying Feed Flowrate

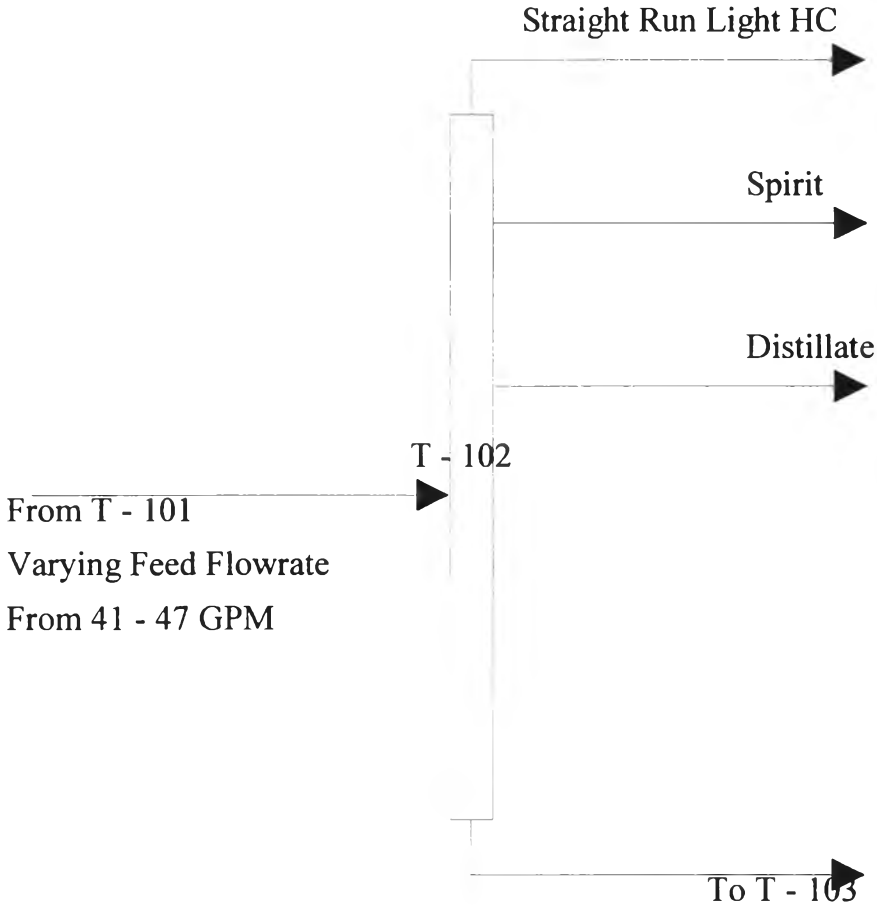

Figure 8.7 Drawing of T-102.

8.2.1 The Effects of Varying Feed Flowrate on Straight Run Light Hydrocarbon

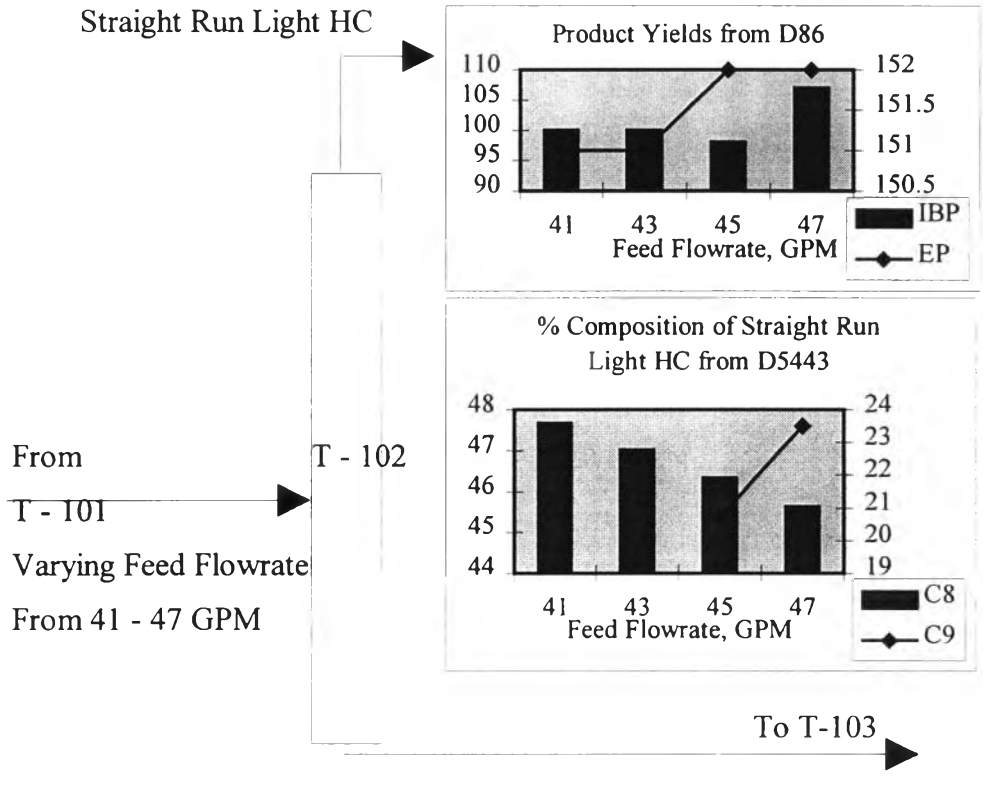

Figure 8.8 Drawing of T-102 (Top of Column).

From experiment, increasing the feed flowrate at constant feed inlet temperature is similar to decreasing the feed inlet temperature, resulting in a heavier fraction at the bottom of the first distillation column. It is correlating to heavier fraction in second distillation column. This probably low feed inlet temperature was not high enough to the evaporate the heavy fraction, resulting in a subtle change of product fraction.

8.2.2 The Effects of Varying Feed Flowrate on Spirit

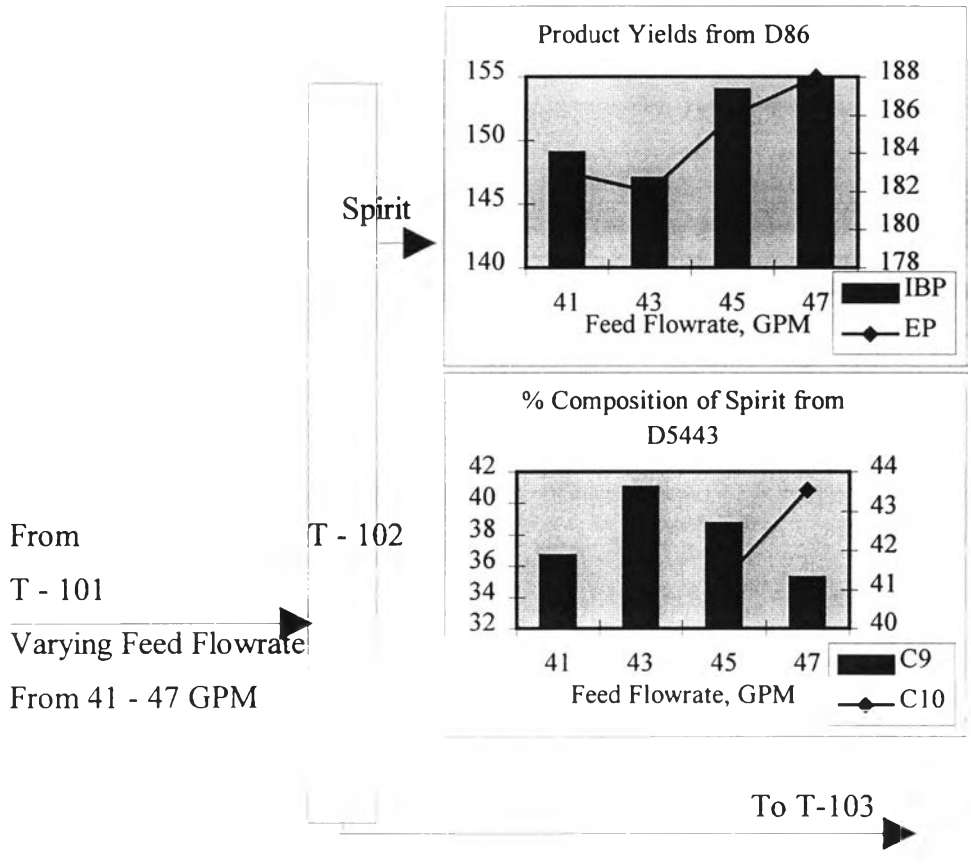

Figure 8.9 Drawing of T-102 (First Side Draw).

For both curves of Spirit shown in Figure 8.9, increasing feed flowrates correlate with a heavier product fraction. It is interesting to note that this product was obtained from the second distillation column, which might suggest that a heavy fraction could not be evaporated to the top of column, leading to a heavier fraction maintained for the first side draw.

8.2.3 The Effects of varying Feed Flowrate on Distillate

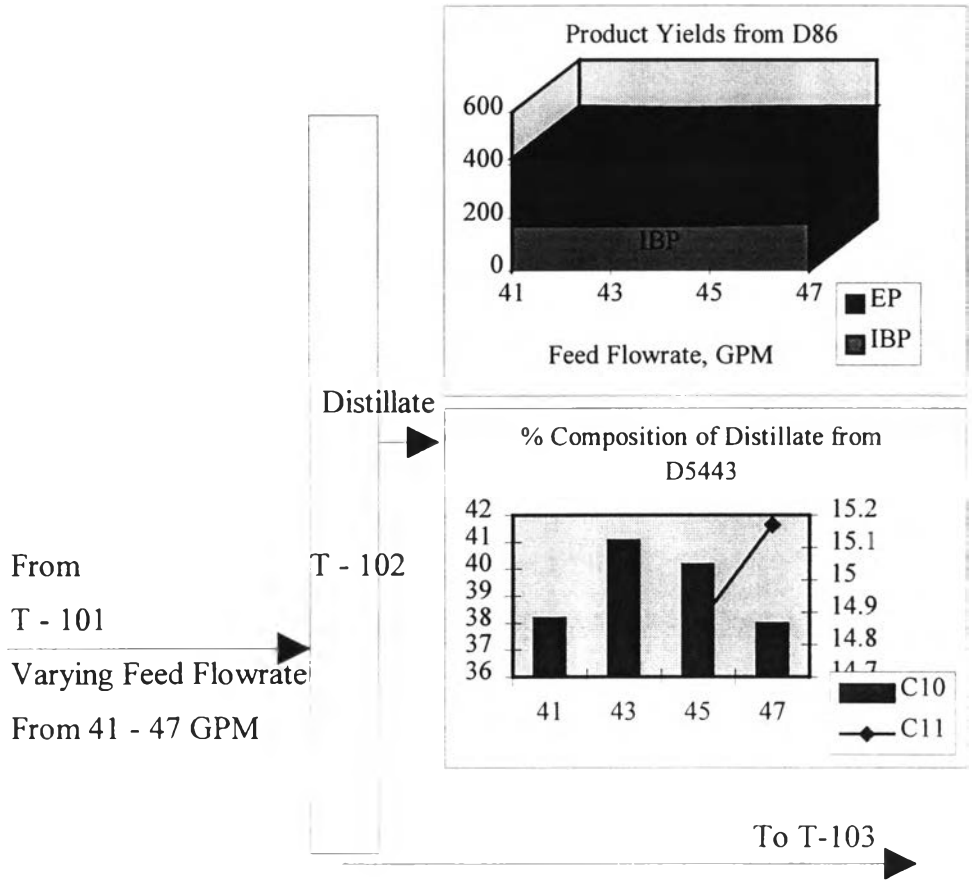

Figure 8.10 Drawing of T-102 (Second Side Draw).

Results shown in Figure 8.10 are similar to those for Spirit.

8.3 The Effects of Varying Reflux Feed Rate

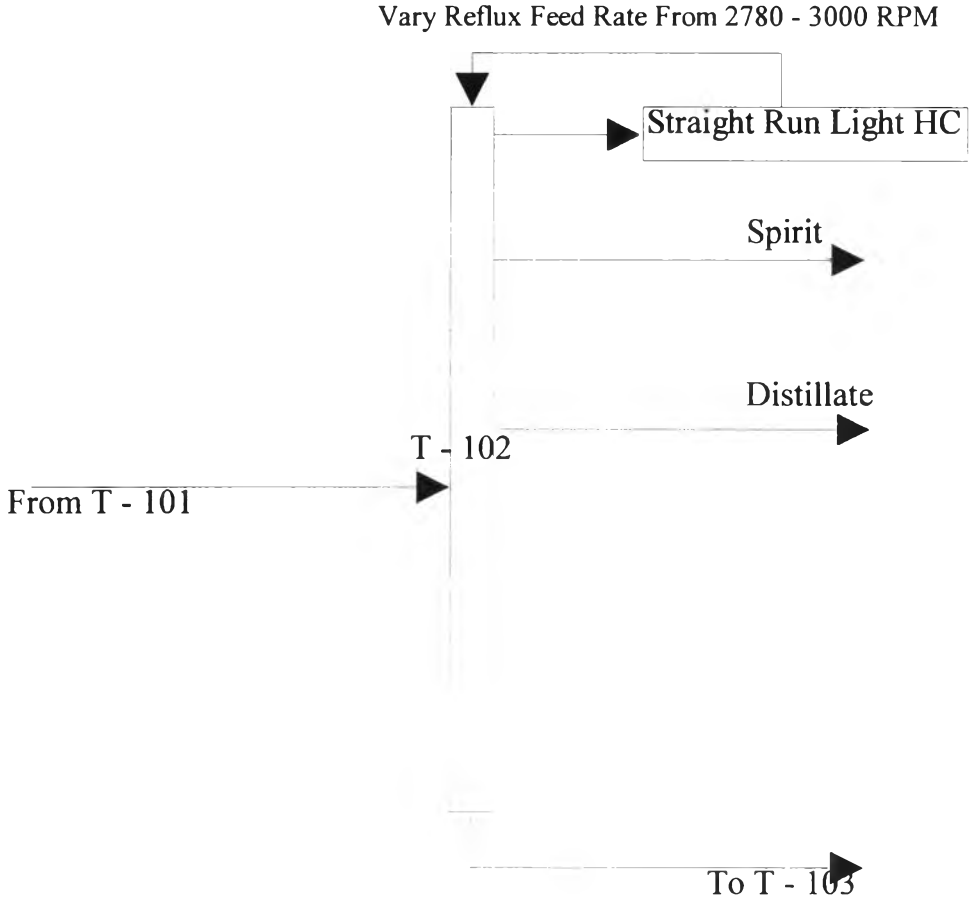

Figure 8.11 Drawing of T-102 on reflux feed rate.

8.3.1 The Effects of Varying Reflux Feed Rate on Straight Run Light Hydrocarbon

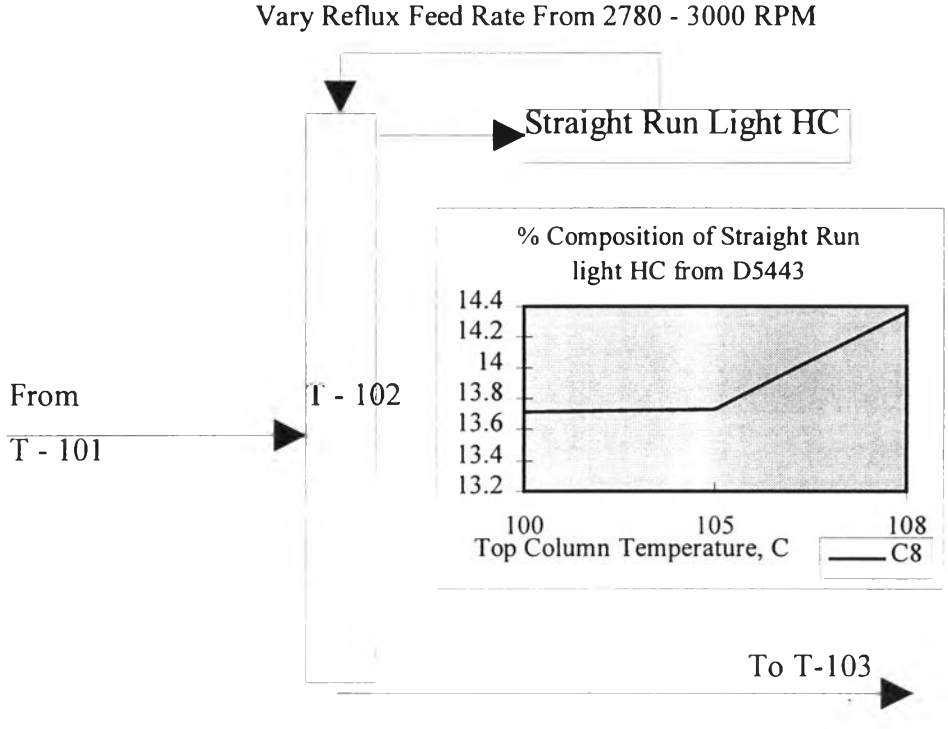

Figure 8.12 Drawing of T-102 (Top of Column).

The dominant hydrocarbon component in Straight run Light Hydrocarbon, as shown in Figure 8.12, is the C8 fraction. A decrease in the pump speed correlates with a decrease in reflux feed rate, and results in a temperature increase at the top of the column. This causes heavy fractions to be evaporated to the top of the column, resulting in a heavier fraction of the product.

8.3.2 The Effects of Varying Reflux Feed Rate on Spirit

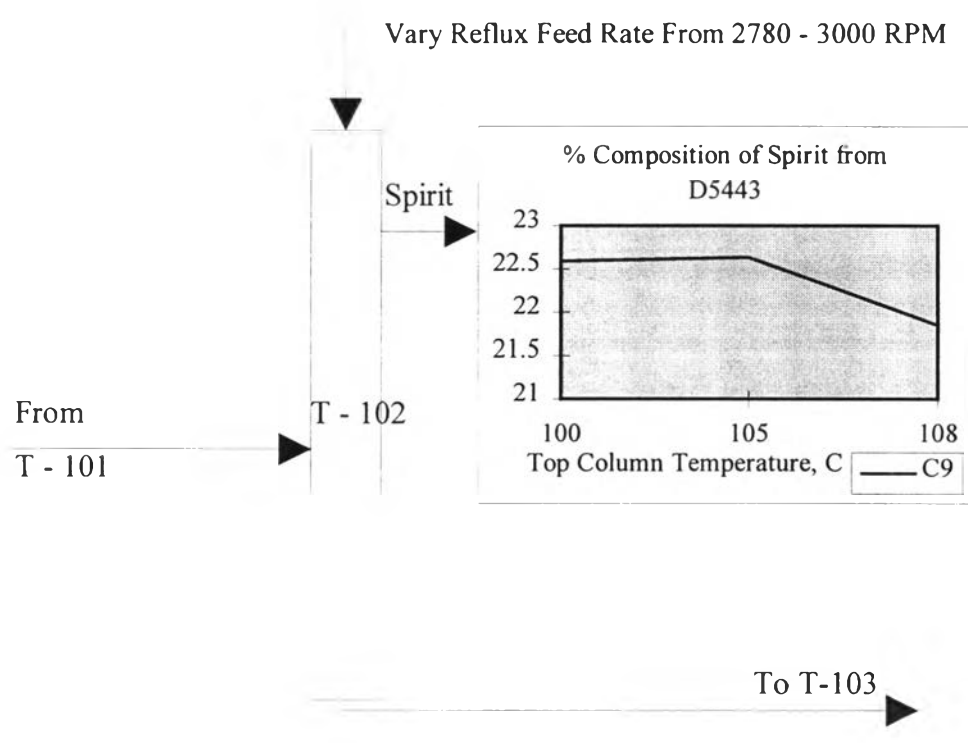

Figure 8.13 Drawing of T-102 (First Side Draw).

From the Straight Run Light Hydrocarbon trend of Figure 8.12, the Spirit fraction would be lighter, resulting in lighter fraction of first side draw product, as shown in Figure 8.13.

8.3.3 The Effects of Varying Reflux Feed Flowrate on Distillate

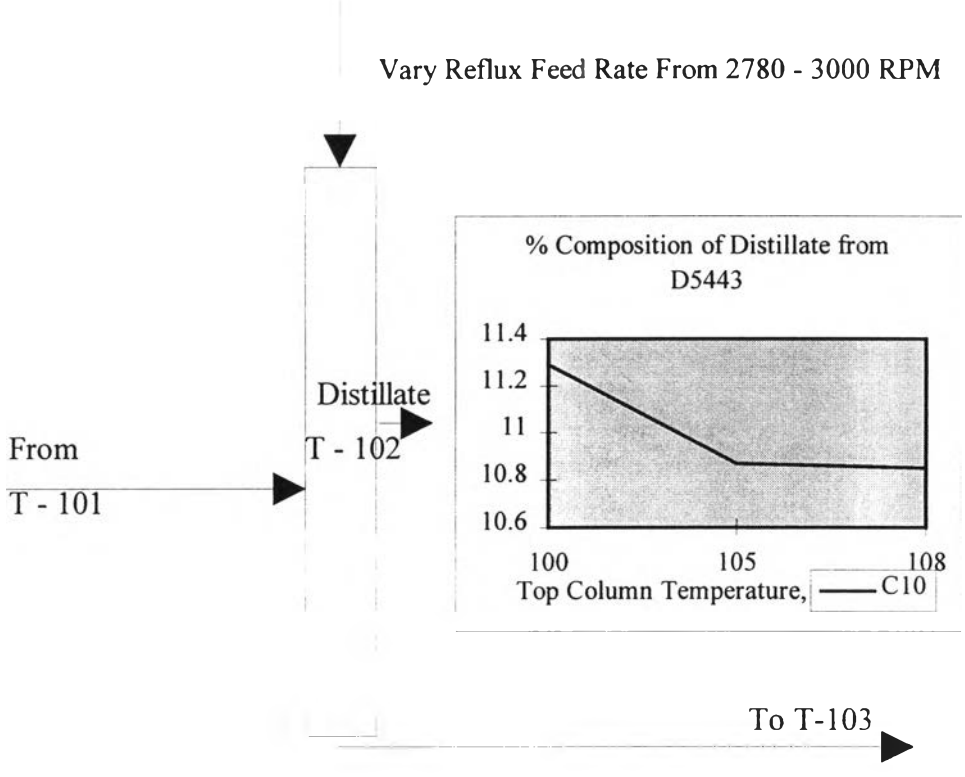

Figure 8.14 Drawing of T-102 (Second Side Draw).

Results for Distillate shown in Figure 8.14 are similar to those for Spirit shown in Figure 8.13.

8.4 Comparison of ΔH from GC PIONA Analysis and Theory

Table 8.1 Comparison of ΔH^*_{GC} and ΔH^*_{Theory}

Feed Inlet Temperature (°C)	Rubber Solvent		Straight Run Light HC		Spirit		Distillate	
	ΔH_T	ΔH_{GC}	ΔH_T	ΔH_{GC}	ΔH_T	ΔH_{GC}	ΔH_T	ΔH_{GC}
125	5,559	5,162	6,748	2,623	2,979	725	5,162	169
130	5,961	7,059	8,644	6,941	3,209	3,823	5,426	629
135	4,636	3,779	7,020	5,716	3,625	11,387	6,439	11,428
150	5,493	8,394	8,723	2,747	3,698	1,493	6,714	1,186

* Unit in Joules

Table 8.2 The Efficiency of Distillation Tower 101 and 102 on ΔH_{GC}

Feed Inlet Temperature (°C)	Rubber Solvent	Straight Run Light HC	Spirit	Distillate
	Efficiency (%)			
125	92.87	38.87	24.33	3.28
130	118.43	80.30	119.44	11.59
135	81.53	81.42	314.13	177.48
150	152.81	31.49	40.37	17.67

Note : Percent efficiencies are greater than 100%, this might because of the error of instrumental machines. This should be corrected by the correction factor of their instruments.

8.4.1 Efficiency of T-101 (by Enthalpy Change of Rubber Solvent)

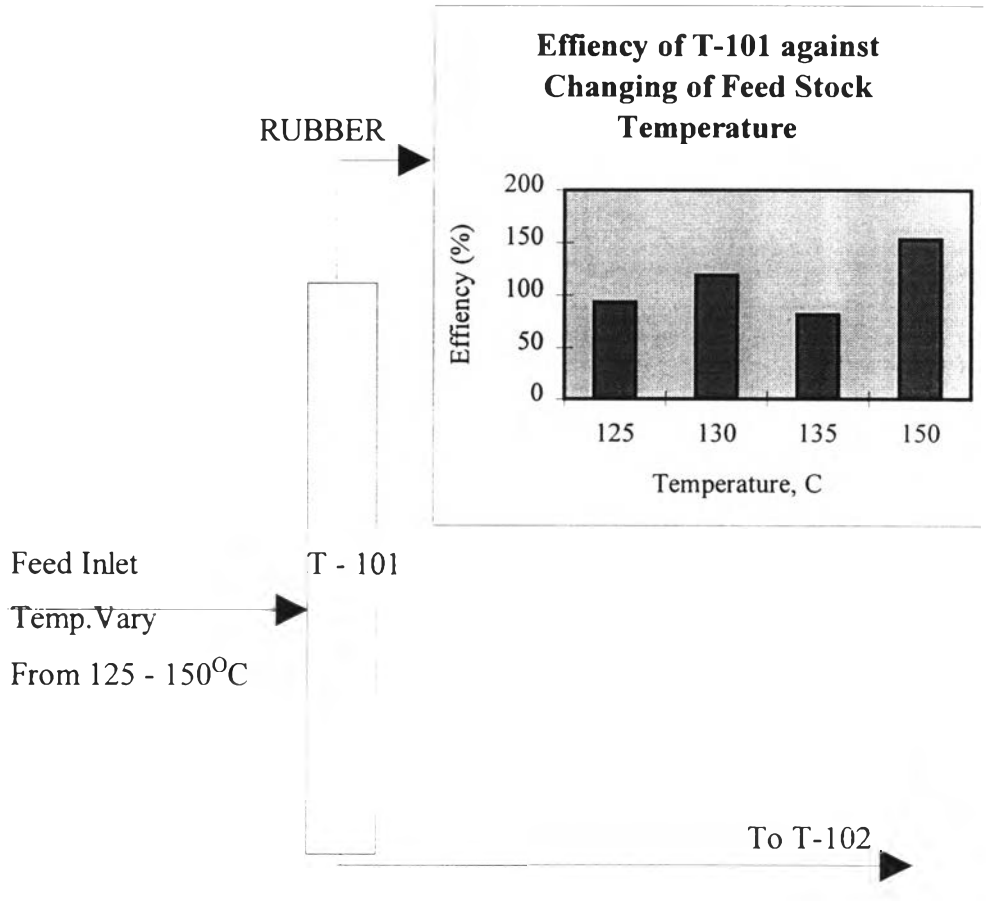

Figure 8.15 Drawing of T-101 on efficiency comparison.

8.4.2 Efficiency of T-102 (by Enthalpy Change of Straight Run Light Hydrocarbon)

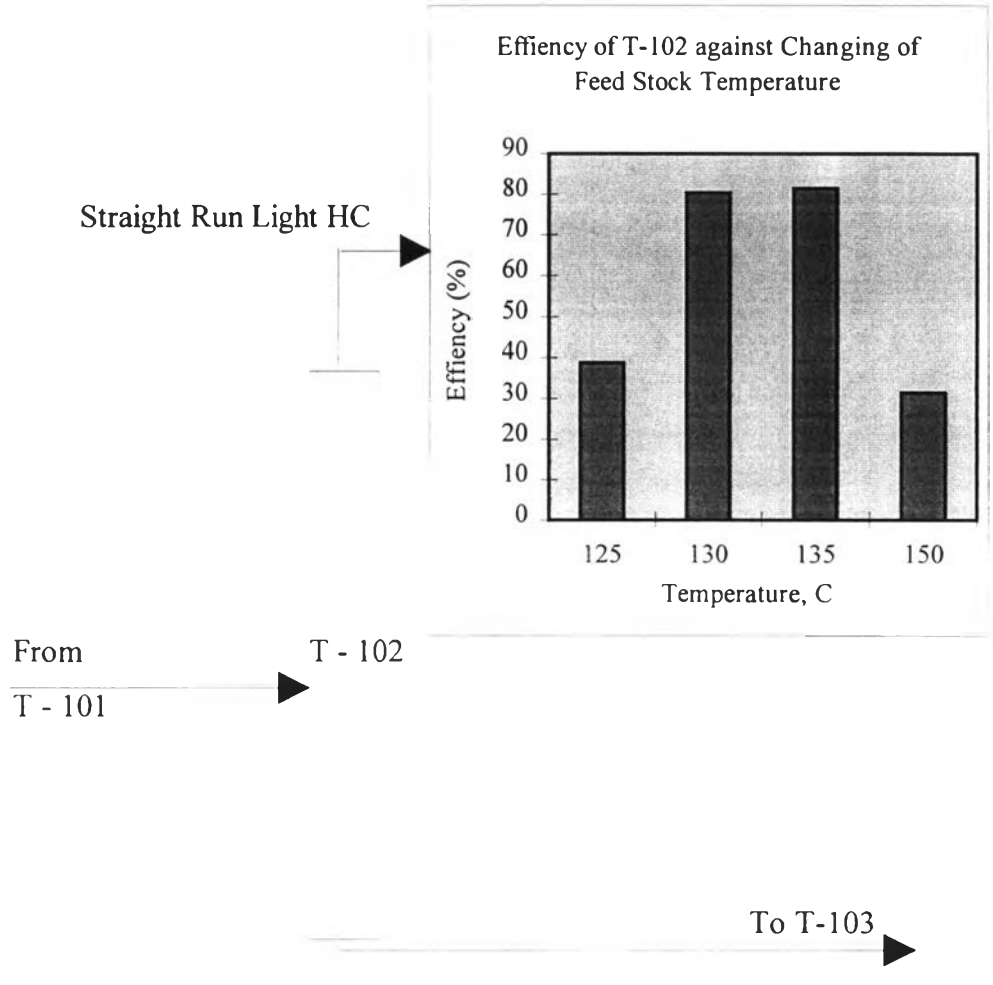

Figure 8.16 Drawing of T-102 on efficiency comparison.

8.4.3 Efficiency of T-102 (by Enthalpy Change of Spirit)

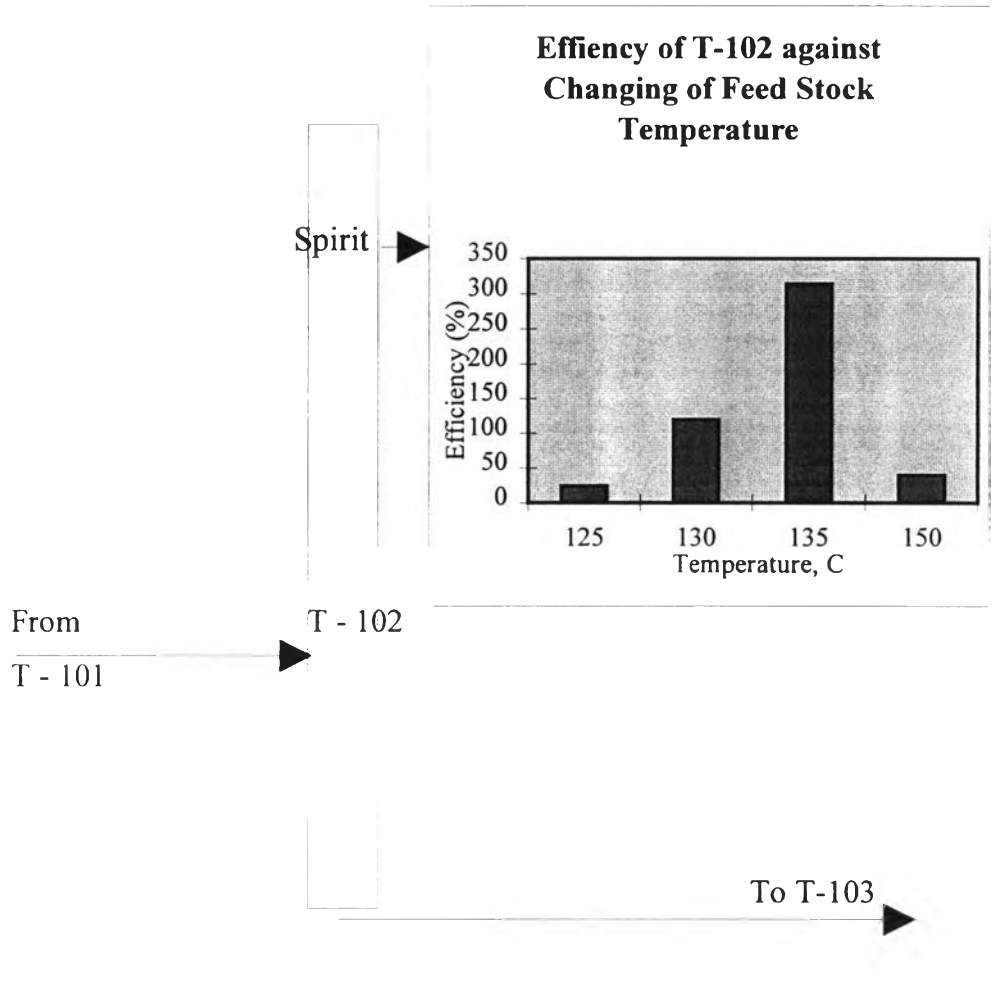

Figure 8.17 Drawing of T-102 on efficiency comparison.

8.4.4 Efficiency of T-102 (by Enthalpy Change of Distillate)

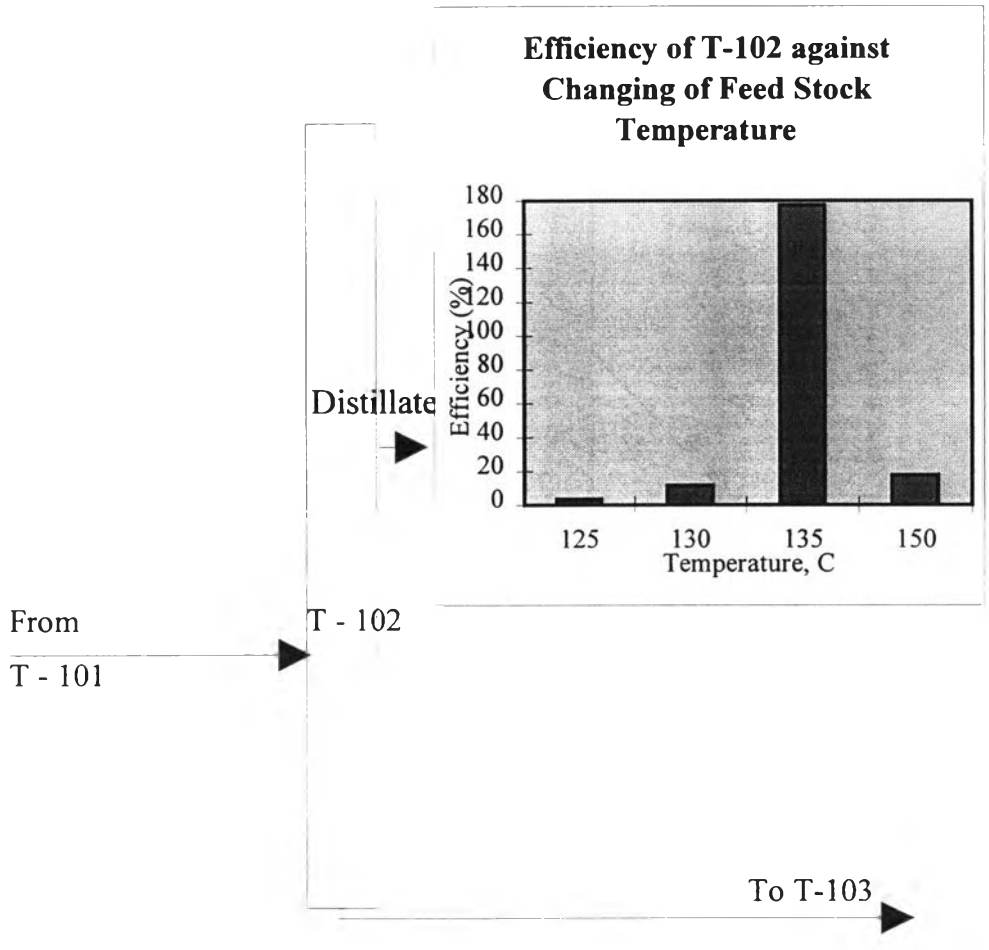

Figure 8.18 Drawing of T-102 on efficiency comparison.

8.5 Optimization the Efficiency of Tower Distillation by Changing of the Feedstock Temperature

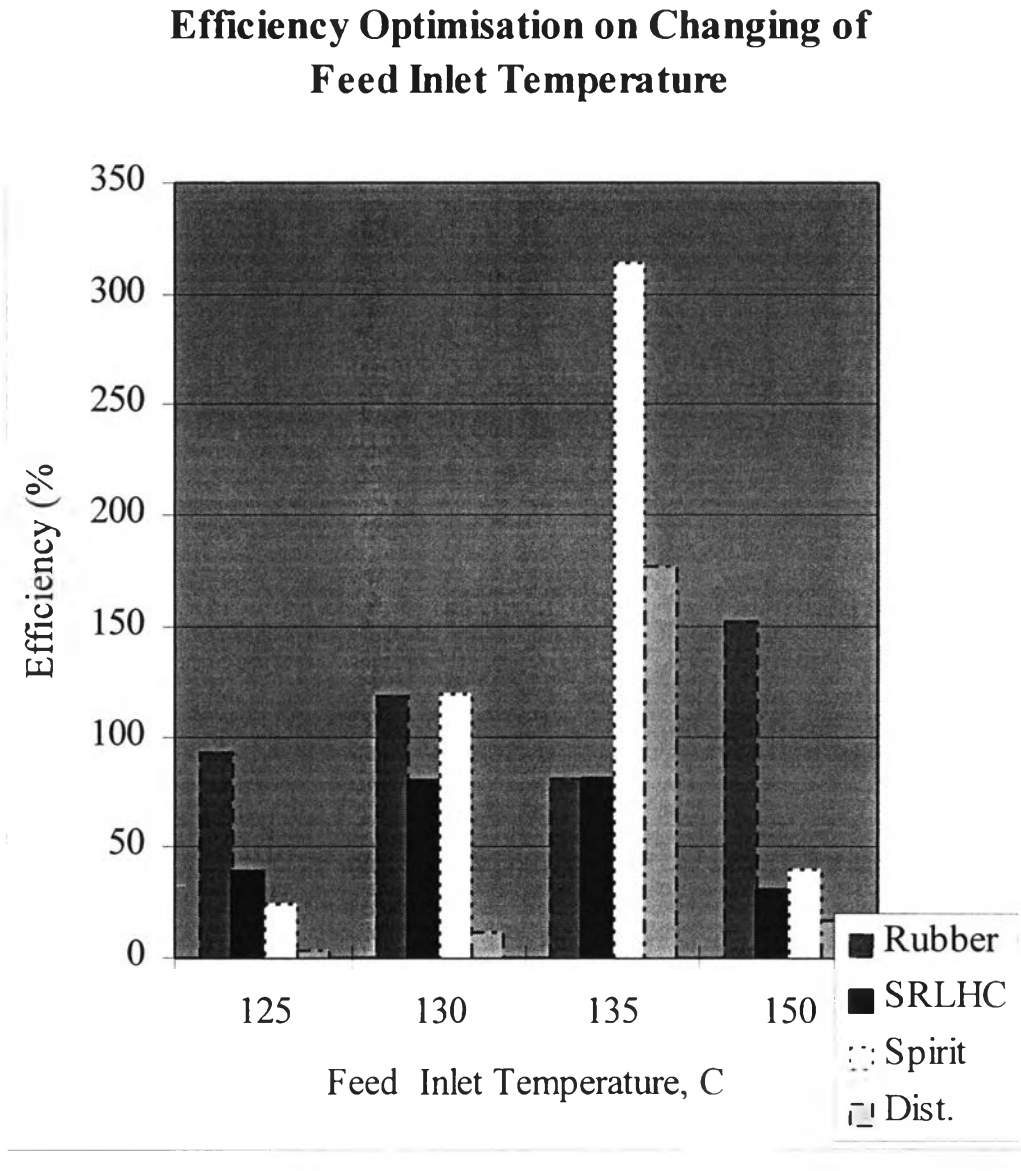

Figure 8.19 Efficiency optimization on changing of feed inlet temperature.

8.6 Optimization the Efficiency of Tower Distillation on All Product Yields

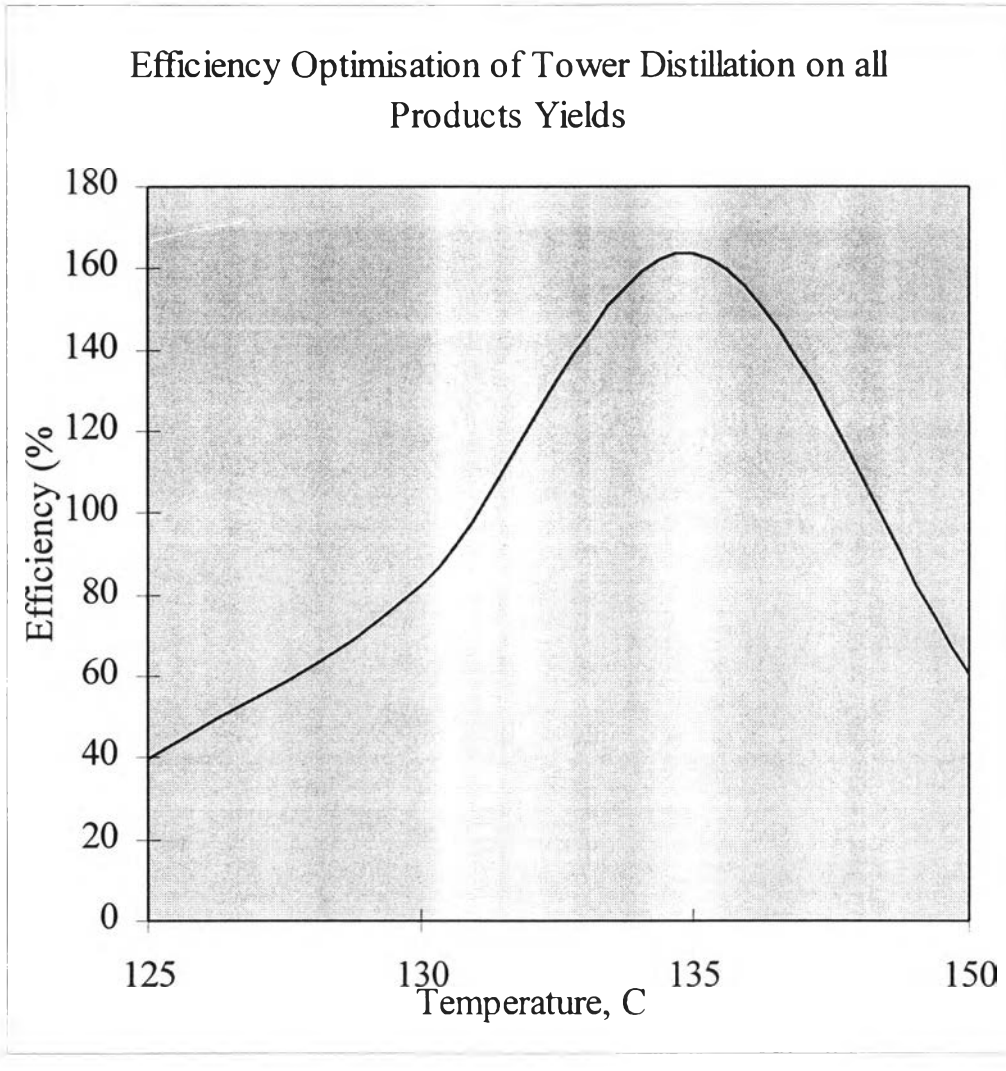

Figure 8.20 Efficiency optimization on changing of feed inlet temperature on all product yields.

As shown in the efficiency optimization curve in Figure 8.20, the highest efficiency of the process is for operation in the range of 130 - 135 ^{o}C.